Continuous measurements of volatile gases as detection of algae crop health

Jon S. Sauer[a,1], Ryan Simkovsky[b,1], Alexia N. Moore[a], Luis Camarda[a], Summer L. Sherman[a], Kimberly A. Prather[a,c], and Robert S. Pomeroy[a,2]

[a]Department of Chemistry and Biochemistry, University of California San Diego, La Jolla, CA 92093; [b]Department of Biological Sciences, University of California San Diego, La Jolla, CA 92093; and [c]Scripps Institution of Oceanography, University of California San Diego, La Jolla, CA 92093

Edited by Alexis T. Bell, University of California, Berkeley, CA, and approved August 25, 2021 (received for review April 20, 2021)

Algae cultivation in open raceway ponds is considered the most economical method for photosynthetically producing biomass for biofuels, chemical feedstocks, and other high-value products. One of the primary challenges for open ponds is diminished biomass yields due to attack by grazers, competitors, and infectious organisms. Higher-frequency observations are needed for detection of grazer infections, which can rapidly reduce biomass levels. In this study, real-time measurements were performed using chemical ionization mass spectrometry (CIMS) to monitor the impact of grazer infections on cyanobacterial cultures. Numerous volatile gases were produced during healthy growth periods from freshwater *Synechococcus elongatus* Pasteur Culture Collection (PCC) 7942, with 6-methyl-5-hepten-2-one serving as a unique metabolic indicator of exponential growth. Following the introduction of a *Tetrahymena* ciliate grazer, the concentrations of multiple volatile species were observed to change after a latent period as short as 18 h. Nitrogenous gases, including ammonia and pyrroline, were found to be reliable indicators of grazing. Detection of grazing by CIMS showed indicators of infections much sooner than traditional methods, microscopy, and continuous fluorescence, which did not detect changes until 37 to 76 h after CIMS detection. CIMS analysis of gases produced by PCC 7942 further shows a complex temporal array of biomass-dependent volatile gas production, which demonstrates the potential for using volatile gas analysis as a diagnostic for grazer infections. Overall, these results show promise for the use of continuous volatile metabolite monitoring for the detection of grazing in algal monocultures, potentially reducing current grazing-induced biomass losses, which could save hundreds of millions of dollars.

chemical ionization | crop protection | volatile organic compounds | algal grazers

Microalgae are prokaryotic or eukaryotic photosynthetic organisms that can grow rapidly in a variety of conditions at large scales. Their efficiency in producing large amounts of biomass in small spaces with few added resources, as compared to terrestrial crops such as corn or soybeans, makes microalgae a promising, sustainable platform for bioproduction of fuels or industrial products. In addition to the most sought-after product, biodiesel, microalgae can also be utilized for production of other valuable fine chemicals such as dyes, cosmetics, pharmaceuticals, and food additives (1–3). Alternatively, microalgae can also be used in tandem with other industrial processes such as removal of dissolved nutrients from wastewater and CO_2 removal from flue gases or the atmosphere (4, 5). Algal research to date has focused extensively on improvements in crop productivity, including strain selection, nutrient control, and management of physiochemical parameters (pH, temperature, etc.). Toward this goal, many cultivators use high-volume open raceway ponds (ORPs) as opposed to more expensive laboratory-style photobioreactors (PBRs) (6). While the cost of algal biomass from ORPs is approximately an order of magnitude lower than PBRs, a key disadvantage is the elevated risk from contamination by unwanted grazers, such as ciliates, rotifers, viruses, bacteria, and fungi (7, 8). Recent estimates of commercial monocultures in ORPs have found grazer-initiated crop failures reduce 10 to 30% of produced biomass, resulting in losses in the hundreds of millions of dollars (9). Part of the challenge posed by grazer contamination involves their ability to rapidly eradicate a microalgae culture, sometimes within 48 h of contamination (10). A component of proper integrated pest management is the utilization of technologies that can rapidly detect grazers at the earliest time at the lowest pest concentrations possible (11). Once the grower is informed of an infection, they can choose to treat the culture to kill or slow the growth of the contaminant, if complementary grazer identity information is available, or immediately harvest to salvage the crop (3).

The detection of grazers has been approached using many analytical methodologies (3, 12, 13). Microscopy and automated optical techniques, such as flow cytometry, have made progress in detecting grazers at low concentrations (<10 units/milliliter) (14, 15). These techniques, while simple and cost-effective, are off-line, can be slow to operate, and require specific protocols or knowledge of the grazer's appearance. Alternatively, technologies from molecular biology, such as qPCR, have shown promise in definitively identifying grazers, with theoretical detection limits of a single molecule; however, challenges associated with cost and producing a library of primers specific to harmful grazers are significant limitations (12, 16). Notably, both methods are highly vulnerable to sampling biases, in which the preference of some grazers to localize on surfaces or on biofilms precludes identification, as most samples are taken from the liquid bulk.

Significance

Wide adoption of algae cultivation to produce environmentally sustainable biofuels and fine chemicals is currently hampered by large losses (10 to 30%) incurred by grazer infections. We show the usage of real-time chemical ionization mass spectrometry to rapidly identify gaseous indicators of grazer infections in cyanobacteria cultures. Grazing was detected significantly faster (up to 3 d) using real-time mass spectrometry than the current methods of microscopy and qPCR. By employing this technology, cultivators may be empowered to treat grazer infestations sooner, thereby protecting the crop and enhancing profitability.

Author contributions: J.S.S., R.S., K.A.P., and R.S.P. designed research; J.S.S., R.S., A.N.M., L.C., and S.L.S. performed research; J.S.S., R.S., K.A.P., and R.S.P. analyzed data; and J.S.S. wrote the paper.

The authors declare no competing interest.

This article is a PNAS Direct Submission.

[1]J.S.S. and R.S. contributed equally to this work.

[2]To whom correspondence may be addressed. Email: rpomeroy@ucsd.edu.

This article contains supporting information online at https://www.pnas.org/lookup/suppl/doi:10.1073/pnas.2106882118/-/DCSupplemental.

Published October 1, 2021.

Recently, attention has been directed to the suite of volatile gases emitted from microalgae as they progress through their bloom life cycle (17–19). For algae, volatile gas emissions are mediated by their environmental conditions or biological state, such as exponential growth, nutrient availability, photooxidative stress, and senescence (17). Furthermore, the presence of bacteria has been shown to transform and modulate the production of volatile gases and metabolites by microalgae (20, 21). Collectively, the microalgae "volatilome" represents a reflection of the organism's state of health (SoH) and, due to the significant effect of grazing on microalgae health, a reflection of the infection state of the bloom. Development of techniques and instrumentation to measure the microalgae volatilome, therefore, represents an opportunity to identify grazer infections in a highly sensitive and descriptive manner (17). Furthermore, issues of sampling biases are less problematic, as volatile gases partition through solutions far better than physical grazers that are fixed to container surfaces. Currently, the predominant technique for analysis of the algae volatilome has been gas chromatography mass spectrometry (GC/MS). While extremely sensitive and effective for identification of volatile gases, common GC/MS systems are not well suited for continuous, in situ measurements without significant modifications (22). In addition, the dominant sampling technique for microalgae volatile gases, solid phase microextraction (SPME), often requires long equilibration times of up to 24 h to obtain sufficient signals (17). Unfortunately, such long sampling times not only delay detection but can average out transient, and potentially important, changes in volatile gas concentrations. Given the fast timescales (1 to 2 d) within which grazer infections occur, there is a need for a headspace monitoring technique with high time resolution and the ability to expediently switch between and measure multiple vessels.

Chemical ionization mass spectrometry (CIMS) is a chemically selective method frequently utilized in the atmospheric, food, medical, defense, and drug enforcement disciplines for the online detection of various gas phase species that are spatiotemporally heterogenous in concentration (23). In CIMS, an ionized reagent gas is mixed with a continuously sampled stream of gas from the sample headspace. Favorable chemical energetics between the reagent ions and analyte molecules in the sample headspace result in soft ionization of the analytes, which then are detected by various types of mass spectrometry. Notably, this method can bypass the need for a gas chromatography column, as the selection of a particular reagent ion (e.g., H_3O^+, $C_6H_6^+$, or I^-) can be used to select for specific classes of molecules while precluding interferences from the major constituents of air (N_2, O_2, CO_2, Ar, CH_4, etc) that are normally ionized by electron impact in GC/MS (24). The removal of the separation step enables the measurement of ambient gases in a highly continuous (1 Hz or faster) manner, while the soft nature of chemical ionization limits ion fragmentation, which can overcomplicate the mass spectra of unseparated gases. Studies of volatile gas emissions from natural marine and freshwater systems using the most common form of chemical ionization, proton transfer reaction mass spectrometry (PTR-MS), have indicated the ability of CIMS to identify distinct states of biogenic activity from phytoplankton and bacteria (25, 26). These findings suggest that CIMS may possess the ability to monitor highly concentrated algal monocultures and benefit from the far higher throughput than modern GC/MS technology. Indeed, the usage of CIMS and PTR-MS has been applied to the continuous monitoring of fermentive bioprocesses and in detection of crop herbivory by unwanted parasites among dozens of other use cases (27–30).

In this study, we use CIMS to monitor freshwater cyanobacterial monocultures of *Synechococcus elongatus* PCC 7942 before and after the addition of a field-isolated ciliate grazer, *Tetrahymena*. Over a 28-d experiment, three 20-L carboys were monitored continuously by CIMS with commensurate biological measurements as they proceeded through healthy growth and were sequentially infected with *Tetrahymena*. Switching between sampling vessels on a 15-min interval allowed the probing of algal volatile gas production at time resolutions higher than previously used, enabling direct comparisons of the ability of gas analysis to detect grazer infections compared to traditional techniques. Analysis of the CIMS data revealed unique insights into the timescales of gas production that highlight the potential for high temporal resolution gas analysis of SoH and grazer infections in microalgae cultures.

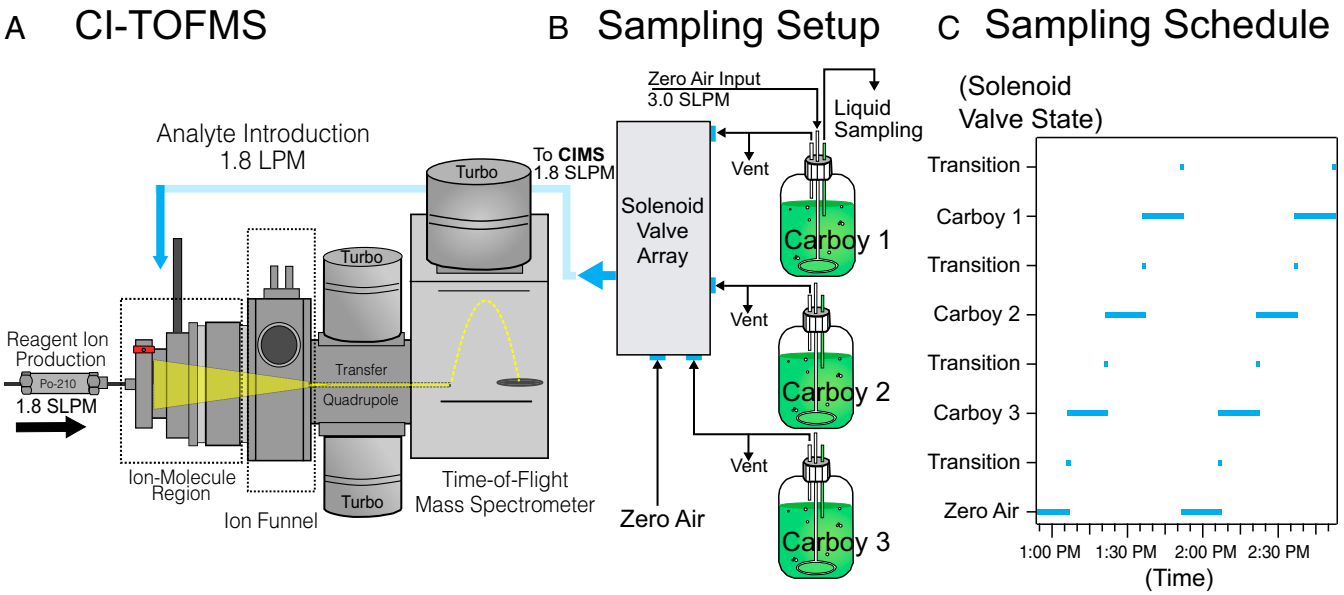

Fig. 1. Experimental arrangement of carboy infection experiments. (*A*) Diagram of the CIMS instrument, (*B*) carboy sampling setup with solenoid valve array, (*C*) example sampling schedule of the solenoid valve array for switching between carboys for CIMS headspace sampling.

Results

Experimental Setup. To demonstrate the capabilities of CIMS analysis on SoH and grazer infections of cyanobacteria, we simultaneously monitored three 20-L carboy cultures of *S. elongatus* PCC 7942, hereafter referred to as PCC 7942, through axenic exponential growth and subsequent planned infections with a field-isolated *Tetrahymena* that rapidly grazes on PCC 7942. For comparison, liquid samples were collected from each carboy at least once daily for microscopy, absorbance spectroscopy, and fluorescence spectroscopy. Upon addition of the predator, the infected carboy was also monitored using a continuous fluorescence spectroscopy system. Cultures were continuously bubbled with sterile zero air, which pushed headspace gases above the culture to a custom-built solenoid valve array that was programmed to switch every 15 min between each of the three carboys and a direct zero-air input (Fig. 1*B*). The headspace or zero-air sample source enabled by the solenoid valve array was pulled directly into the ion-molecule region (IMR) of a chemical ionization time of flight mass spectrometer, in which the continuous flow of air from the carboys or zero air was ionized by $(H_2O)_nH^+$, which proceeds by proton transfer, and directly introduced into the CIMS without any column chromatography (Fig. 1*A*). Mass spectra were accumulated as a sum of 60,000 spectra collected over 1 s (Fig. 1*C*).

Mass Spectral Characteristics of PCC 7942. The mass spectra collected from the headspace over the PCC 7942 cultures displayed numerous peaks indicative of volatile gases present in the samples. Fig. 2*A* shows a comparison of average mass spectra obtained from both the headspace of Carboy 1 and clean zero air during a period of axenic algal growth on the fourth day after PCC 7942 inoculation. The mass spectrum for both sample types is dominated by the water cluster reagent ions at mass to charge ratios (*m*/*z*) 19, 37, 55, 73, and 91, which are typical clusters formed in chemical ionization. In all carboys, the remainder of the mass spectrum is composed of numerous ions generated by proton transfer (M+1), which fall between *m*/*z* 40 and 200. At this time point, the fraction of ion intensity occupied by nonwater cluster ions was 7% for zero air and 11% for the headspace of Carboy 1, in which total ion count (TIC) was ~2.5×10^6 counts per second. The ratio of ion intensity for nonwater cluster ions between Carboy 1 and zero air was 1.51. Of this ion intensity, Carboy 1 possessed 75 unique *m*/*z*'s that were 25% greater in average intensity than zero air, suggesting their origin from either cyanobacterial production, the BG-11 growth medium, or the carboy assembly. Of these 75 unique *m*/*z*'s, 49 ions were found to exhibit distinct time-variant behavior over the course of Carboy 1's experimental lifetime, for which time-variant behavior is defined operationally as a >10% increase or decrease in normalized intensity over the timescale of the experiment. Time series that showed exponential decay from the outset of the experiment or spikes caused by pressure instabilities were excluded from this analysis, indicating that the 49 ions that changed intensity over the course of the culture's lifespan were most likely due to active biogenic processes and not off-gassing from the media or experimental arrangement. These results together demonstrate the ability of water cluster CIMS to detect a wide range of unique volatile gases that can be related to the health of cyanobacterial and other microalgae cultures.

Of the ions detected by the CIMS, direct assignments of several more intense species were made utilizing complementary MS methods such as solid phase microextraction gas chromatography mass spectrometry (SPME-GC/MS) and modified atmospheric pressure chemical ionization high-resolution mass spectrometry (APCI-Orbitrap) incorporating recent innovations for direct analysis of gas phase species (31) (Protocol S1). These identifications are listed in *SI Appendix*, Table S1. Overall, molecular formulae or putative identifications were made for a small fraction, <15%, of the total number of ions observed by CIMS during the experiment duration. Many of these species were observed to be aliphatic ketones and aldehydes similar to those observed in investigations of algae by others (17, 18, 32–34); however, nitrogen-containing gases, including ammonia and C_4H_7N, were an important constituent of the headspace, which has been generally overlooked by previous analyses of commercial algal volatile gases despite evidence of the production of methylated amines from phytoplankton in natural seawater (33, 35, 36).

Evaluation of Tubing and CIMS Inlet Equilibration Times. While CIMS used in this work possesses a relatively low-mass resolution (~1,200 full width at half maximum) and does not induce significant ion fragmentation that can be used for molecular identification, valuable analyte information can be obtained through monitoring the rise or decay time of an ion as the CIMS switches between sampling vessels. This rise or decay time (*SI Appendix*, Fig. S2) can be modeled using a double exponential fit and the resultant time for the ion to reach $1/e^2$(86.5%) of its equilibrated intensity can be calculated (37, 38). The $1/e^2$ decay times are reflected as the sum of multiple physical processes as gases travel down the length of the tubing from the sample source to the instrument IMR inlet. Molecules with a high saturation concentration (volatility) remain in the gas phase, which results in short equilibration times between samples. Conversely, low volatility molecules tend to stick to tubing and result in longer equilibration times (37). In addition to saturation concentration, smaller molecules with high dipole moments, such as

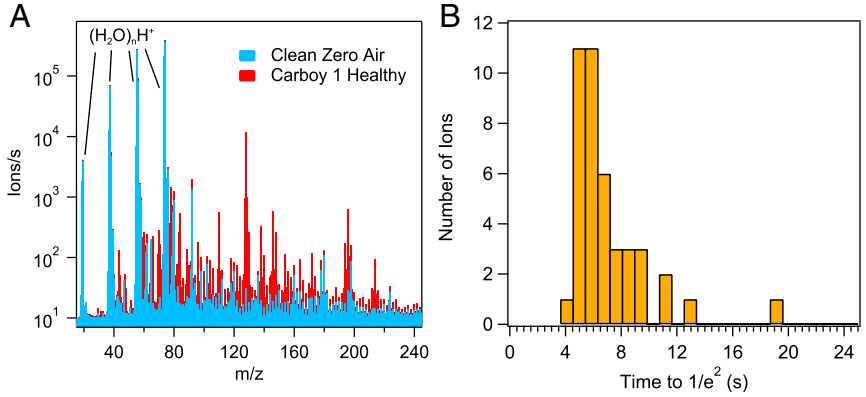

Fig. 2. (*A*) Average CIMS mass spectrum for zero air and Carboy 1 headspace. (*B*) The $1/e^2$ histogram of ion equilibration times obtained from switching between sampling zero air and Carboy 1.

NH_3 or HCl, may partition into water microlayers on tubing walls, thus increasing their equilibration times significantly (38). Together, an analysis of gas rise or decay times, in combination with their corresponding *m*/*z*'s, provides valuable information as to the general chemical characteristics of the observed ions. This analysis also enables calculation of the minimum time the CIMS must monitor a sampling vessel before it can switch to the next vessel.

We applied this analysis to a set of 42 unique *m*/*z*'s using rise or decay times as the CIMS switched between sample carboys and zero air. The results of this analysis performed on data acquired on the fourth day after inoculation of Carboy 1 with PCC 7942 are shown in Fig. 2*B*, with the single omission of the $1/e^2$ value of ammonia (NH_3). Notably, the majority of $1/e^2$ decay times fall under 12 s, comparable with equilibration times necessary for high-speed environmental measurements (39). In contrast, ammonia and other even mass gases at *m*/*z*'s 70 and 76, whose even *m*/*z* values suggest an odd number of nitrogen atoms if ionized by proton transfer [the predominant ionization scheme in $(H_2O)_nH^+$], displayed longer equilibration times (14 and 19 s), with ammonia's $1/e^2$ time being ∼335 s. The assignment of nitrogen in the molecular formulas of these species is consistent with their longer equilibration times, as their pronounced basicity promotes dissolution into water coated on tubing walls. Based on the longest equilibration time of ammonia of 5.6 min, this key operational parameter means that the CIMS, with an appropriate sample switching device, is capable of analyzing 10 different vessels in under an hour. Furthermore, these equilibration times are not fixed and can be further improved through higher flow rates, tubing diameters, heating, and chemical coatings of the tubing or the CIMS inlet. Finally, this analysis demonstrates that the 15-min sampling schedule used in this experiment was more than sufficient to accurately determine ion intensities for a diverse suite of gases present in the culture headspace samples.

Time Series Analysis. Volatile gases from Carboys 1, 2, and 3 were monitored over a total period of 28 d. All carboys were inoculated with PCC 7942 at the same time, and each carboy was sequentially infected on days 8, 13, and 23, respectively, with *Tetrahymena* at a concentration of 0.1 cells/milliliter (Fig. 3, solid vertical lines). This infection density was chosen because it is well below the typical limit of detection (LOD) of microscopy at 5 to 20 cells/milliliter and the theoretical limit of blank for the technique used of 20 cells/milliliter (40–42). Twice daily after infection, liquid samples were taken manually from the infected carboy and analyzed by microscopy for the presence of *Tetrahymena*. Grazers were observed first from each carboy on days 12, 16, and 27 (Fig. 3, dashed vertical lines), with further information on the specific duration until detection summarized in Table 1. While qPCR was not used to detect grazers in these experiments, a separate analysis was performed to assess the LOD of qPCR toward the detection of *Tetrahymena* and is detailed in *SI Appendix*. The observed qPCR LOD of 597.6 cells · mL^{-1} (*SI Appendix*, Fig. S4) for *Tetrahymena* greatly exceeded detection thresholds by microscopy; thus, we chose microscopy for the experiment time course as the benchmark grazer detection method. To observe changes in algal biomass associated with grazing at faster timescales, each grazer inoculated carboy was monitored by continuous fluorescence (Fig. 3*B*) until the complete loss of biomass, as indicated by the daily fluorescence measurements, visible color change and culture collapse (Fig. 3*A*). Continuous fluorescence, while providing a higher temporal resolution in showing biomass loss during the grazer-induced crash, did not confer any significant advantage to grazer detection over manual daily fluorescence sampling. In addition, during the infection of carboy 3, the continuous fluorescence signal began to gradually diminish before changes in the manual daily sampling, likely due to observed biofouling of the sensor at high algal biomass. Optical density (OD) at a wavelength of 750 nm was also monitored daily (*SI Appendix*, Fig. S5). While OD and fluorescence show good agreement in these experiments, fluorescence was chosen as the primary measurement, as it better reflects the presence of live cyanobacteria as opposed to OD, which can capture senescent cells and detritus. Given the agreement between OD and fluorescence, we find that any self-shading during growth likely did not drastically alter chlorophyll production in these experiments, which could distort assessment of culture productivity.

Numerous gases showed significant changes in intensity in response to grazer infection; however, only the time series of the fastest-responding and most intense species will be primarily discussed here. The most significant change in ion intensities were NH_3 at *m*/*z* 18 (Fig. 3*C*) and its associated water cluster adducts at *m*/*z*'s 36 and 54. Initial NH_3 ion intensities were observed to be elevated at the outset of the experiment and are indicative of volatized NH_3 off-gassing from the BG-11 medium, which contains 6 mg/L ferric ammonium citrate, as observed by monitoring sterile BG-11 (*SI Appendix*, Fig. S6). After the first 2 d of algal growth, this NH_3 ion signal decreased by nearly two orders of magnitude and remained below 2×10^4 counts · s^{-1} until after *Tetrahymena* addition. This decrease was likely caused by uptake of ammonium by PCC 7942 as well as gradual ventilation of NH_3 by the bubbled zero air. After grazer addition to each carboy, an initial intensity spike of NH_3 was observed for each carboy on days 11, 15, and 25. Notably, some NH_3 signal carryover from Carboy 1 to Carboys 2 and 3 occurred during Carboy 1's ammonia spike as well as carryover from Carboy 2 to Carboy 3 during Carboy 2's ammonia spike. These carryover events were caused by excess ammonia in the sampling lines and CIMS inlet that did not sufficiently evaporate before the CIMS switched to the next sampling vessel, consistent with the slow equilibration rate observed for ammonia. After the first intensity spike, the NH_3 signal decreased before spiking a second time for each infected carboy in concert with the culture crash and decrease in fluorescence signals. Notably, the magnitude of the first ammonia spike increased in intensity as the experiment duration continued in concert with the increase in algal biomass in later carboys (Fig. 3 *A* and *C*). We tentatively suggest that the magnitude of the first ammonia spike appears to be biomass dependent and may be an algal stress-related response. Although ammonia release has been described for some strains of *Anabaena* (43), though not as a stress or predation response, algal growers have used free ammonia addition as a method to control pests (44). We hypothesize that this initial ammonia spike represents a possible defense mechanism. In contrast to the first spike, the magnitude of the second ammonia spike is relatively consistent for all three carboys, suggesting that its production is a function of biomass degradation caused by the predation of the grazer on the cyanobacteria.

While ammonia signals increased after predator addition, the intensity of *m*/*z* 137, an unidentified monoterpene, showed a clear decrease in Carboys 1 and 2 multiple days before detection of *Tetrahymena* by microscopy (Fig. 3*D*). For Carboy 3, the intense NH_3 signal from the first spike disrupted the ion chemistry of the CIMS, preventing reliable observations of *m*/*z* 137 (*SI Appendix*, Fig. S7). For this reason, in cases in which *m*/*z* 18 intensity exceeded 2,500 counts per second, *m*/*z* 137 intensity was discarded. This protocol was also followed for most other ions except nitrogen-containing (even-mass) ions, which showed stability in intensity during periods of high NH_3. This stability is likely due to the higher gas phase proton affinity of these molecules, which are able to receive protons from NH_4^+ (proton affinity [PA] = 853.6 kJ/mol) if NH_3 had sufficiently titrated $(H_2O)_nH^+$ as the active reagent ion; however, monoterpenes ($PA_{alpha\ pinene}$ = 878 kJ/mol) would not. In Fig. 3*E*, the intensity of *m*/*z* 70, which was determined to have the molecular formula C_4H_7N and is likely 1- or 3-pyrroline (PA = 925.8 or 931.0 kJ/mol)

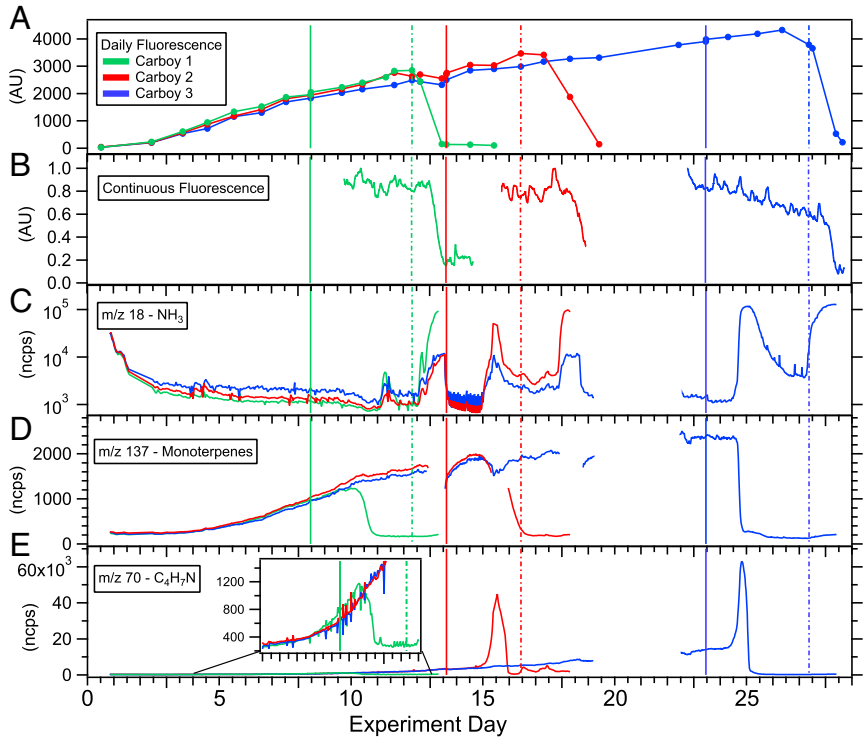

Fig. 3. Time-series data of the carboy experiment colored by carboy (Carboy 1: green, Carboy 2: red, Carboy 3: blue). (*A*) Daily fluorescence: 590 nm excitation/670 nm emission. Arbitrary units, AU. (*B*) Continuous flow-through cuvette fluorescence: 420 nm excitation/670 nm emission. (*C*) CIMS *m/z* 18 (NH_3) intensity normalized counts per second, ncps. (*D*) CIMS *m/z* 137 (monoterpenes) intensity. (*E*) CIMS *m/z* 70 (C_4H_7N) intensity. Solid vertical lines denote the time of *Tetrahymena* addition for each carboy; dashed vertical lines denote the first time of *Tetrahymena* detection via microscopy.

showed strong positive changes in intensity for infected Carboys 2 and 3 but only decreased in intensity in Carboy 1 (Fig. 3 *E*, *Inset*). Similar to the double spike phenomenon observed for NH_3, it appears that the amount of algal biomass present at infection time is an important effector of *m/z* 70 production in response to grazing. These results are further supported by measurements of *m/z* 32, methylamine (PA = 899.0 kJ/mol), which only appeared in response to grazing in Carboy 3, the vessel that reached the highest level of biomass before the grazer-induced crash (*SI Appendix*, Fig. S8). Given the disruption to the $(H_2O)_nH^+$ ion chemistry by NH_3, in these experiments, the authors note that sample dilution is an option for future analyses to counteract titration by NH_3; however, this comes at a compromise of sensitivity to non-NH_3 analytes in the sample stream, which are also diluted.

Volatile Gases as Indicators of Grazing. Having observed volatile gas signatures that change consistently over the growth of all cultures after the introduction of predators, we compared the timing of gas intensity changes as detected by CIMS to indicate the presence of grazers relative to the timing of grazer detection by microscopy and continuous fluorescence. By applying an empirically derived detection threshold based on the ion signal changing by 10σ over a 4-h window, we find that the CIMS detects the impact of grazers 25 to 76 h before microscopy detection, depending on the gas used for detection and the specific experiment (Table 1). C_4H_7N, in all cases, was the first gas to appear or diminish in response to grazing and was effective for use in all three carboys, while monoterpenes are more effective at lower biomass, at which complications from high ammonia were less problematic. Notably, the duration at which grazer detection was achieved by volatile gas analysis decreased over the experimental duration, indicating that the increased biomass in Carboys 2 and 3 seems to have shortened the algal response to infection. For microscopy, detection of grazers after inoculation was quite similar for Carboys 1 and 3; however, it occurred earlier for Carboy 2. High variance in detection time by microscopy is reflective of challenges inherent in the technique at low cell densities, in which statistical fluctuation and heterogeneous localization of the predator may be prominent factors. For example, a 1-mL sample screened for grazers at a detection limit of 1 cell/milliliter may not contain a grazer, even if the bulk grazer concentration is ∼1 cell/milliliter. While continuous fluorescence cannot detect grazers until after cyanobacteria biomass diminishes, the remarkably similar times reflect a grazing consistency between the three carboy inoculations, which help validate chemical comparisons between the three systems.

Table 1. Time after grazer addition before detection technique flags presence of Tetrahymena grazer

Carboy	NH_3 (hours after grazer addition)	Monoterpenes (hours after grazer addition)	C_4H_7N (hours after grazer addition)	Microscopy (hours after grazer addition)	Continuous fluorescence (hours after grazer addition)
1	67	47	45	92	119
2	36	39	32	69	114
3	30	—	18	94	112

For CIMS-measured species, grazer detection was based on a signal intensity change of 10σ over a duration of 4 h. Microscopy identification was at the first date of visible grazers observed during liquid grab sampling. Continuous fluorescence detection was based on a 10σ over a duration of 4 h.

Temporal Changes in Ion Intensity. To better understand if the apparent correlation for changes in volatile gas intensity of some chemical species and increased cyanobacterial biomass is a more generalized phenomenon, we calculated the moving 1-h derivative of ion signals, which changed in response to grazing, and evaluated these signal changes by separate carboy. From an analysis of the maximum raw ion intensity derivative of gases in each carboy (Fig. 4*A*), it is apparent that denser algal cultures produce larger total gas change in response to grazing, suggesting that the utilization of algal gases as a diagnostic will be more effective for denser, mature ponds. In addition, the maximum derivative of each ion was normalized to their respective raw intensities at the time of *Tetrahymena* addition, and then the time for the ion to double in intensity at this rate of change was calculated (Fig. 4*B*).

This calculation allows the investigation of how much, by fraction, each volatile gas changed in time as a response to grazer addition between the three carboys. The results in Fig. 4*B* show that the doubling time for gases significantly decreased from Carboy 1 to Carboy 3, indicating that the quantity of initial algal biomass at time of infection accelerates the production or loss of gases in response to grazing. Furthermore, this observation demonstrates that as the doubling time decreases, the need for higher time resolution analytical methods, such as CIMS, become necessary to capture these signal changes for effective grazer detection in a manner that current GC/MS-based gas analysis techniques simply cannot.

Volatile Gases as Indicators of SoH. While the primary scope of this study focuses on changes to production of gases in grazer-infected algae, we also observed interesting changes in volatile gas intensities during healthy growth of PCC 7942. Shown in *SI Appendix*, Fig. S9*A*, a collection of demonstrative gases in Carboy 1 are plotted across the time series of the experiment. Each of these gases generally increased in intensity with the growth of PCC 7942 in Carboy 1; however, the distinct shape of changes in each ion's intensity during growth demonstrates the biochemical complexities that likely underlie the production of each compound.

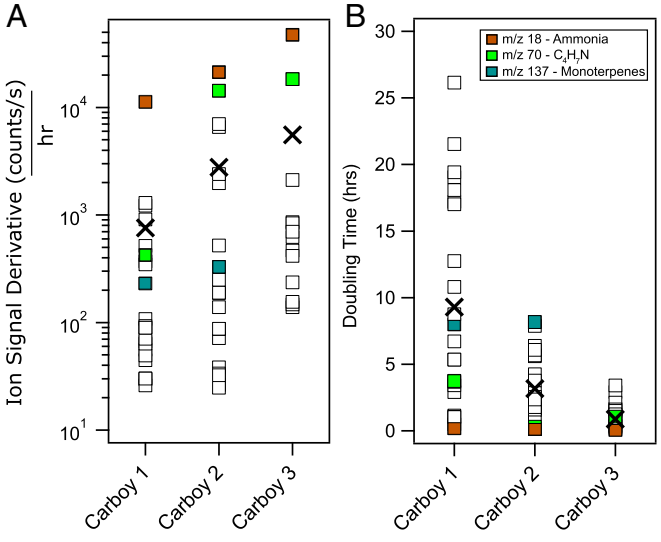

Fig. 4. Derivative analysis of grazer-affected gas production from PCC 7942. (*A*) Maximum derivative value of raw ion signal change. (*B*) Normalized derivative doubling time for the same set of ions in *A*. The × markers designate the average signal derivative and doubling time for each carboy. Selected ions from Fig. 3 are indicated by colored boxes in each panel to emphasize their time-dependent behavior in comparison to other ions observed in this study.

Notably, *m*/*z* 127, 6-methyl-5-hepten-2-one (6-MHO), exhibits a departure from continuous increase with algal growth, plateauing ~5.5 d into the experiment and remaining at approximately the same signal intensity until grazing pressure on PCC 7942 by *Tetrahymena* (added day 8) resulted in loss of productive algal biomass able to produce 6-MHO. As continuous bubbling of the carboys occurred during the full experiment duration, causing continuous ventilation of dissolved gases, a plateau of 6-MHO suggests that algal production of 6-MHO reached a steady-state value that may be biologically informative. Indeed, departure from growth of 6-MHO signal appears to correspond with the changes in the productivity of the algal culture, in which exponential algal growth similarly leveled off at approximately the same time in the experiment time course (*SI Appendix*, Fig. S9*B*). To further compare the production of volatile gases in Carboy 1 with healthy growth, the daily average ion intensity of the chemical species shown in *SI Appendix*, Fig. S9*A* were divided by the daily average algal fluorescence. Shown in *SI Appendix*, Fig. S9 *A*, *B*, *D*–*F*, the ratio of each ion to daily fluorescence decreased to a stable value until algal biomass was degraded by grazing after day 8. A stabilization of ion to fluorescence ratio indicates that the per-cell production rate of these gases likely remained constant. However, the ratio of 6-MHO to fluorescence showed different behavior over the experimental time course, similarly in concert with the departure from exponential growth to attenuated growth (*SI Appendix*, Fig. S9*B*). While assessing the specific biological purpose or reason for the release of each of these volatile gases is beyond the scope of this work, ratios of ion intensity to algal fluorescence help distinguish whether the per-cell production of volatile species varies with increasing biomass. We believe that better distinguishing the roles of biomass-variant and -invariant volatile gases may open many new doors to better understanding algal biochemistry in the future. While further investigation of the connections between PCC 7942 growth and 6-MHO production are warranted, these results suggest that some volatile gases may be used as metabolic indicators of the culture's growth phase, better informing the cultivator of how to manage the algal crop to maintain or change the growth phase to maximize biomass productivity or induce generation of desired products.

Discussion

The utilization of chemical ionization mass spectrometry identified several promising molecular species as diagnostic tracers to identify *Tetrahymena* grazing in PCC 7942. We found that nitrogen-containing gases are highly reliable unique tracers indicative of algal grazing. While the putative identification of all ions was not possible, complementary analyses with GC/MS and atmospheric pressure chemical ionization-high resolution mass spectrometry (APCI-HRMS) were used to obtain further information. However, ascertaining the identity of all volatile gases measured by CIMS is not required for the goal of identifying predation or infection in algal cultures. Provided the *m*/*z*'s measured by the CIMS consistently respond to destructive contamination, knowledge of their identity and biochemical purpose only provides a better understanding of the biochemistry of the system overall. This is analogous to medical measurements of temperature or blood pressure, which are linked to pathogenesis in often unknown and highly complicated systems that can be used to indicate a change in the health of the patient.

Furthermore, this study evaluates and compares volatile gas measurements with standard monitoring techniques, such as microscopy and spectroscopy, in terms of critical time-based metrics that include 1) time to detection following a below-LOD infection, which reflects the sensitivity of the method to either the number or level of grazing activity of the contaminant, or 2) time of detection prior to a culture crash, which is an important criteria for growers, as it determines how much time is available to prevent or recuperate potential biomass losses. The data provided in Fig. 3 and

Table 1 demonstrate the improved performance of the real-time measurements of the CIMS over microscopic and spectroscopic monitoring methods, with volatile gas analysis of grazer-infected PCC 7942 cultures providing detection signatures, at minimum, 24 h faster than microscopy and up to 3 d faster for the experimental conditions discussed herein. While the type of custom CIMS used in this work with $(H_2O)_nH^+$ chemistry was effective in detecting grazer infections, other types of chemical ionization instruments, such at proton transfer reaction mass spectrometry (PTR-MS) and selected ion flow tube mass spectrometry (SIFT-MS), should be similarly useful. Both PTR-MS and SIFT-MS are commercially available, albeit expensive, systems but have enhanced capabilities for wider selectivity and reduced humidity dependence.

We further identify fascinating features regarding the timescale and intensity with which volatile gases are produced in response to grazing that appear linked to algal biomass. First, we observed transient early signal changes whose intensity increases change disproportionately with increased biomass in each carboy. For example, the peaks of the first ammonia burst in Carboys 1 and 2 differ by ~25× in maximum intensity (Fig. 3*C*, Days 11.5 and 15.5), while the fluorescence or OD changes are both 1.1× . Based on the transient and disproportionate biomass-dependent nature of this response, we have hypothesized that this feature is unlikely to be caused directly by degradation of biomass or increased encounter rates but instead may represent a defense response that is nonlinearly amplified by denser cell populations. The possibility that algae respond to stressful stimuli in a population-dependent manner, as has been observed in the literature to abiotic stress (45), indicates that gas analysis as a diagnostic method will likely require multiple data types to contextualize the overall SoH of the algal crop. Second, we observed that overall signal changes occur earlier when infection occurs at a higher initial biomass density (Fig. 4). Because this phenomenon is more generally observed with all volatile signals investigated, including nontransient signals, its cause is more likely a direct consequence of biomass degradation and is related to increased encounter rates in higher-density cultures, which are subsequently compounded by increased predator replication and grazing rates. Interestingly, though, microscopy and fluorescence detection times did not change in a similar manner. The ability of ponds to respond to stressful stimuli in a population-dependent manner informs us that gas analysis as a diagnostic method will likely require multiple data types to contextualize the overall SoH of the algal crop. We furthermore leveraged our high-temporal resolution measurements to show that changes in gas composition due to grazing occur on a <24-h basis, with some intensities changing by a factor of 2 or more in less than an hour. The sampling frequency of a volatile gas diagnostic measurement for algae likely needs to occur more than once daily and ideally as frequently as once hourly or more, which is not easily done for GC/MS, the typical method that is used in such studies. Given the constraints imposed by partitioning of volatile gases to sampling tubing, we find that CIMS can monitor ~10 vessels per hour, which will be improved through modifications of the sampling arrangement for field application, greatly offsetting the cost of this higher-complexity instrumentation. Future applications of this approach to algal monitoring will significantly benefit from higher-complexity numerical analyses that can draw connections between algal gas production and various other indicators of health toward the goal of giving cultivators the ability to "decide" a pond is infected in an automated manner. The grower may then initiate a predetermined intervention in an automated fashion to minimize biomass losses like those observed in these experiments and in the field. Given reports of regular losses in the field of 30% or greater in biomass production and the 1 to 3 d of prior notice to any significant biomass loss that is possible within the CIMS system, we believe that the CIMS monitoring system could effectively allow a grower time to recover nearly all of the biomass lost, even using the most drastic intervention of harvesting the entire system.

Future work on this method will require the study of multiple algae–grazer pairs to assess the specificity of volatile gas responses to grazing. Given that many microalgae are known to produce different volatile metabolites, it is likely that some chemicals may be unique to algae–grazer pairs (17). Other gases, likely simpler molecules like NH_3 that are derived from common precursors such as proteins, will probably be conserved among many algae–grazer combinations. Development for future field applications will need to address sampling of unwanted outdoor contaminants that could confound analysis of volatiles from the crop. Here, we envision the usage of sampling interfaces, which provide a large surface area of pond water sampled by a stream of clean air, which will be measured by CIMS. This method will, at minimum, protect the system from drastic changes in gas intensity carried by local airborne sources but is still vulnerable to gaseous compounds that may partition into ponds over time. Diagnostic markers of grazer infection will therefore need to be carefully selected based on the risks of external contamination by similar or isobaric compounds. While the analysis in this study focuses on a volatile gas assessment for the health of microalgae, it is important to note that chemical ionization mass spectrometry can be used to monitor health-indicating gases in many other production systems, including beer, cheese, monoclonal antibodies, and laboratory-grown meats, all of which require stringent cleanliness.

Materials and Methods

Culture Conditions. *S. elongatus* PCC 7942 was grown for maintaining *Tetrahymena* or for inoculations for larger cultures in BG-11 medium (46) in 250-mL or 2-L flasks with continuous shaking (125 rpm) at 30 °C under continuous illumination of 200 μmol photons · m^{-2} · s^{-1} from fluorescent cool white bulbs.

***Tetrahymena* Isolation and Culturing.** A 30-L BG-11 culture of *S. elongatus* PCC 7942 grown in a 100-L polybag at the University of California San Diego Greenhouse Biology Field Station, as described by Schoepp, et al. (47), had crashed due to an unknown contaminant. A sample of this crashed culture was brought into the laboratory and analyzed by light microscopy, through which it was observed that the predominant organism was a free-swimming ciliate. This culture sample was serially diluted or manually isolated under microscopic visualization into flask cultures of PCC 7942 or into wells of a flat-bottom multiwell cell-culture dish (Costar, Corning) containing dense *S. elongatus* cultures as diluents to first isolate the grazer and subsequently to culture the grazer. Grazer cultures were incubated at 30 °C under low light conditions (10 μmol photons · m^{-2} · s^{-1}) or more routinely at room temperature under ambient light conditions. In contrast to healthy PCC 7942 cultures, grazed cultures were yellow, resulted in visible clumping of the few remaining *S. elongatus* cells, and were predominantly composed of ciliates when viewed by light microscopy on a dissecting microscope. A 1-μL sample of a grazed culture was used as a template for Q5 (New England Biolabs) PCR amplification of the ITS2 region using the ITS1 (5′-AGGAGAAGTCGTAACAAGGT-3′) and ITS4 (5′-TCCTCCGCTTATTGATATGC-3′) primers, producing an ~600-bp band. PCR was performed according to the Q5 standard protocol, with an annealing temperature of 55 °C and an elongation time of 3 min and 45 s. The PCR product was purified using the Zymo DNA Clean & Concentrator-5 kit and sequenced by Sanger sequencing with the ITS1 primer. The resulting sequence was analyzed by Basic Local Alignment Search Tool to determine the closest identified species as *Tetrahymena tropicalis, Tetrahymena thermophila,* or *Tetrahymena rostrata*.

Carboy Cultures and Sampling Setup. Three 20-L transparent polycarbonate carboys (Nalgene) fitted with a custom inlet/outlet polypropylene cap with stainless steel bulkhead compression fittings sealed with Viton O-rings for gastight liquid and gas sampling designed to prevent the unwanted introduction of organisms from the ambient environment were filled with 18 L BG-11 and autoclaved (*SI Appendix*, Fig. S1). Once cooled, the carboys were inoculated with 2 L *S. elongatus* PCC 7942 cultures previously grown in 2-L flasks to an OD at 750 nm of 0.08 to 0.1 so that the carboys were inoculated to an OD at 750 nm of ~0.01. Carboys were connected to sampling devices as shown in Fig. 1 and *SI Appendix*, Fig. S1. Cultures were grown continuously under cool (4,100 K) fluorescent light, starting at 135 μE incident radiation at

the front face of each carboy and increased to 190 μE after 24 h of growth, at which time self-shading lowered the risk of photobleaching. *Tetrahymena* were added at a calculated concentration of 0.1 cells/milliliter separately to Carboys 1, 2, and 3 after 8, 13, and 23 d following culture inoculation, respectively.

Clean zero air, obtained from a generator (Sabio 1001) and regulated by a mass flow controller (Alicat) to 3 standard liters per minute (SLPM) was directed through a 47-mm 0.2-μm polytetrafluoroethylene filter into each carboy, in which the air input line was terminated at a submerged circular length of perforated 1/4″-outside diameter perfluoroalkyl (PFA) tubing so that all input air was released as bubbles directly into the culture. This construction distributed bubbles throughout the carboy to adequately mix and supply air to enable culture growth. Liquid samples were collected from the carboy using a manifold of three-way and one-way check valves connected by Tygon tubing to the compression fittings on the cap, all of which were autoclaved attached to the carboy at the time of media preparation. The valve manifold allowed sanitation of liquid sample lines by 70% ethanol with significantly reduced backflow risk of ethanol or microorganisms into the carboy. The output headspace gas from each carboy flowed through 3.175-mm inside diameter PFA tubing into a custom Labview controlled four-channel solenoid valve array, which switched between each carboy and clean zero air on a 15-min sampling cycle (Fig. 1*C*). Sample air from the solenoid array was drawn in by the CIMS at a fixed flow rate of 1.8 SLPM, with excess sample gas overflowing to a downward-pointing exhaust port for condensed water droplets to drain (Fig. 1*B*).

Ultra-high-purity N_2 gas, produced by boil-off from a liquid nitrogen dewar, was bubbled through a 250-mL Pyrex bottle filled with liquid chromatography mass spectrometry purity H_2O at 2.2 SLPM. Humidified N_2 exiting the bottle was passed into a Po-210 α-particle source (20 mCi) to produce protonated water clusters, $(H_2O)_nH^+$, where $n = 1,2,3,\ldots$, that were mixed with sample air in the IMR of the CIMS instrument ($P_{IMR} = 23$ Torr). Input flow of sample and reagent gas into the IMR was controlled by inline critical orifices (O'Keefe) at 1.8 SLPM for both flows. Chemical ionization of analytes in the IMR by protonated water clusters proceeds through several possible reaction mechanisms, which are controlled by the chemical energetics of the analytes and reagent ion. These reactions are detailed in Eqs. 1–**4** (39),

$$M + X^+ \rightarrow M^+ + X \quad \text{Charge Transfer} \qquad [1]$$

$$M + HX^+ \rightarrow MH^+ + X \quad \text{Proton Transfer} \qquad [2]$$

$$MH + X^+ \rightarrow M^+ + HX \quad \text{Hydride Abstraction} \qquad [3]$$

$$X^+ + M + Z \rightarrow MX^+ + Z \quad \text{Adduct Formation,} \qquad [4]$$

where M is the analyte, X is the reagent, and Z is a third body required to carry away excess energy. For $(H_2O)_nH^+$, it is assumed that the predominant reaction channel is through proton transfer, which occurs when the proton affinity of the analyte exceeds that of the water cluster. For $(H_2O)_nH^+$, the range of proton affinities for $n = 0,1,2,3$ water clusters is 691, 694, 730, and 769 kJ · mol^{-1} respectively; however, it is difficult to predict the true distribution of water clusters in the IMR, as the observed mass spectrum may not reflect this directly (48). Given the relatively high pressure of the IMR, water clusters are expected to reach the equilibrium cluster distribution far faster than their residence time (~100 ms) in the IMR.

In chemical ionization, the humidity inside the reaction chamber can drastically affect the distribution of ions and the dynamics of chemical ionization, which often requires humidity-dependent calibration or internal standards to account for changes in sample humidity (24). While humidity of the sampling lines was not monitored during these experiments, the temperatures of the sampling lines were held constant at 30 °C, with the carboys in a temperature-controlled laboratory at 23 °C. In previous experiments, which did not use tubing heating, significant challenges with condensation were encountered. From this, we assume that the tubing stayed quite close to the saturation humidity. Furthermore, an analysis of the water cluster ions over the duration of one of the carboy experiments (*SI Appendix*, Fig. S10) also showed that the ratios of water cluster ions were quite stable against each other. Given a large change in humidity, we might expect to see these ratios drift toward larger clusters if more humid, and smaller clusters if less.

After ionization, reagent and product ions were passed further into the instrument, starting with an electrodynamic ion funnel ($P_{IF} = 0.3$ Torr), which radially confined ions using a radio frequency (RF) pseudopotential applied across 30+ concentric brass plates of decreasing diameter. Ions transmitted through the funnel were passed into an RF-only transfer quadrupole ($P_{Quad} = 5 \times 10^{-5}$ Torr), which directs the ions into the final chamber: a commercial orthogonal extraction time-of-flight mass spectrometer ($P_{ToF} = 4.0 \times 10^{-7}$ Torr) with chevron microchannel plate detector (Tofwerk AG) (Fig. 1*A*). Approximately 60,000 mass spectra were averaged per second on an analog-to-digital converter and transferred to computer storage for later analysis. For the analyses in this work, the mass spectral window was limited between 10 and 400 *m/z*, as there was a dearth of ions observed above this mass range. Mass resolution was ~1,200 full width at half maximum for the spectra obtained in this experiment. MS data were baselined, calibrated, and analyzed in Tofware, a graphical user interface plugin for Igor Pro-7. Time series data of unit-mass *m/z*'s were averaged into ~15-min bins to reduce data density and were separated by the carboy sampled using a complementary mask file generated by the solenoid valve array. Approximately 5 min of MS data acquired at the beginning of each time bin was discarded to remove signal that was equilibrating between samples.

Biological measurements. *Tetrahymena* cell counts were obtained by manual counting ciliates present in 1- to 10-μL droplets of culture on a microscope slide under a dissecting microscope with 25× objective and 10× eyepiece. Alternatively, for low-density grazer cultures, 200 μL culture in a 96-well plate could be rapidly scanned using the same dissecting microscope setup. For all cell counts, at least five individual sample counts were collected and averaged to calculate the cell density of the culture or inoculum.

Manually collected cyanobacterial culture samples were analyzed by OD at 750 nm in a clear, plastic cuvette or by absorbance and fluorescence spectroscopy of a 200-μL sample in a 96-well plate using a TECAN Infinite M200 plate reader to collect OD_{750} values and autofluorescence values at an excitation of 590 nm and emission of 670 nm.

Culture samples were checked for bacterial and fungal contamination by spotting 5-μL of sample on BG-11 Omni plates (BG-11 with 0.04% glucose, 5% Luria broth, and 1.5% agar) and incubating the plate in the dark at 30 °C overnight (49). All *S. elongatus* flask and carboy cultures were demonstrated to be free of contaminants prior to *Tetrahymena* addition.

Continuous Fluorescence. After each carboy was inoculated with *Tetrahymena* grazer, a low-flow (~1 mL/minute) peristaltic pump was connected and withdrew carboy liquid through 1/8″ outside diameter Tygon tubing to a quartz 1-cm^2 flow-through cuvette before returning the liquid back to the carboy in a closed loop. The cuvette was placed in a custom fabricated fluorescence spectrometer, which irradiated the cell with 420 nm light produced by a photodiode laser (Thorlabs). An orthogonally oriented photodiode detector (Thorlabs) with a 650-nm high-pass filter measured fluorescence, which was logged at a rate of 1 Hz by a Labview interface. Continuous fluorescence data were background subtracted, normalized, and averaged into 10-min intervals after experiment completion.

Gas Chromatography Mass Spectrometry of Grazer-Infected PCC 7942. The 10-mL crimp cap vials were filled with 4 mL BG-11 growth media, 4 mL previously grown culture of PCC 7942 at an OD of ~0.25, or 4 mL PCC 7942 culture with ~370 *Tetrahymena* cells added. Vials were crimp sealed and held under fluorescent light for the experiment duration. For each microalgae–grazer experiment, 10 vials were prepared, of which 5 were controls of algae only and 5 were infected at the experiment start with *Tetrahymena* ciliate. Each day of the experiment, an untested vial from each group was sampled by SPME fibers possessing a 50-μm stationary phase of divinylbenzene/Carboxen/polydimethylsiloxane (solid gray, Supelco) equilibrated in the vial headspace for 24 h. Samples were analyzed on an Agilent Technologies 7820A/5975 GC/MS using an Agilent BP5 column. The following GC/MS parameters were utilized for analysis of SPME fibers: inlet temperature: 250 °C; splitless injection, carrier flow: 2 mL · min^{-1}; GC temperature program: 35 °C for 3 min, then +7 °C · min^{-1} to 230 °C, which was held for 2 min; MS transfer line temperature: 260 °C; MS scan range: *m/z* 32.5 to *m/z* 300 over 1 s. MS data were baselined using the statistics-sensitive nonlinear iterative peak-clipping algorithm (50) and analyzed in OpenChrom (51) (https://lablicate.com/platform/openchrom). MS spectra were identified using the NIST14 Electron Ionization mass spectral database. Results were subsequently exported to Igor Pro-7 (Wavemetrics) for plotting.

Data Availability. Comma Separated Value (CSV) and raw Hierarchical Data Format (HDF) data have been deposited in the University of California San Diego Library, https://doi.org/10.6075/J0GH9GHW (52).

ACKNOWLEDGMENTS. We thank Joseph Manson for assistance in building the hardware and software for the valve manifold and Joseph Mayer for assistance in building the custom carboy caps. We thank Kerry Kizer, Laura Lowe, and Paul Kasrazadeh for helpful assistance in preparing cultures for the experiments herein. This material is based on work supported by Department of Energy Grant DE-EE0007094.

1. N. G. Schoepp, W. Wong, S. P. Mayfield, M. D. Burkart, Bulk solvent extraction of biomass slurries using a lipid trap. *RSC Adv.* **5**, 57038–57044 (2015).
2. E. Christaki, E. Bonos, I. Giannenas, P. Florou-Paneri, Functional properties of carotenoids originating from algae. *J. Sci. Food Agric.* **93**, 5–11 (2013).
3. L. T. Carney, T. W. Lane, Parasites in algae mass culture. *Front. Microbiol.* **5**, 278 (2014).
4. A. D. Kroumov *et al*., A systems approach for CO2 fixation from flue gas by microalgae—Theory review. *Process Biochem.* **51**, 1817–1832 (2016).
5. M. Molazadeh, H. Ahmadzadeh, H. R. Pourianfar, S. Lyon, P. H. Rampelotto, The use of microalgae for coupling wastewater treatment with CO2 biofixation. *Front. Bioeng. Biotechnol.* **7**, 42 (2019).
6. D. Klein-Marcuschamer, Y. Chisti, J. R. Benemann, D. Lewis, A matter of detail: Assessing the true potential of microalgal biofuels. *Biotechnol. Bioeng.* **110**, 2317–2322 (2013).
7. T. M. Mata, A. A. Martins, N. S. Caetano, Microalgae for biodiesel production and other applications: A review. *Renew. Sustain. Energy Rev.* **14**, 217–232 (2010).
8. V. L. Harmon *et al*., Reliability metrics and their management implications for open pond algae cultivation. *Algal Res.* **55**, 102249 (2021).
9. J. W. Richardson *et al*., A financial assessment of two alternative cultivation systems and their contributions to algae biofuel economic viability. *Algal Res.* **4**, 96–104 (2014).
10. I. Moreno-Garrido, J. P. Cañavate, Assessing chemical compounds for controlling predator ciliates in outdoor mass cultures of the green algae Dunaliella salina. *Aquac. Eng.* **24**, 107–114 (2000).
11. R. C. McBride *et al*., Contamination management in low cost open algae ponds for biofuels production. *Ind. Biotechnol. (New Rochelle N.Y.)* **10**, 221–227 (2014).
12. F. Di Caprio, Methods to quantify biological contaminants in microalgae cultures. *Algal Res.* **49**, 101943 (2020).
13. P. Deore, J. Beardall, S. Noronha, Non-photochemical quenching, a non-invasive probe for monitoring microalgal grazing: Influence of grazing-mediated total ammonia-nitrogen. *Appl. Phycol.* **1**, 32–43 (2020).
14. J. G. Day, N. J. Thomas, U. E. M. Achilles-Day, R. J. G. Leakey, Early detection of protozoan grazers in algal biofuel cultures. *Bioresour. Technol.* **114**, 715–719 (2012).
15. H. I. Forehead, C. J. O'Kelly, Small doses, big troubles: Modeling growth dynamics of organisms affecting microalgal production cultures in closed photobioreactors. *Bioresour. Technol.* **129**, 329–334 (2013).
16. P. M. Letcher *et al*., Characterization of *Amoeboaphelidium protococcarum*, an algal parasite new to the cryptomycota isolated from an outdoor algal pond used for the production of biofuel. *PLoS One* **8**, e56232 (2013).
17. K. E. Achyuthan, J. C. Harper, R. P. Manginell, M. W. Moorman, Volatile metabolites emission by in vivo microalgae—An overlooked opportunity? *Metabolites* **7**, 39 (2017).
18. K. L. Reese *et al*., Chemical profiling of volatile organic compounds in the headspace of algal cultures as early biomarkers of algal pond crashes. *Sci. Rep.* **9**, 13866 (2019).
19. C. L. Fisher, P. D. Lane, M. Russell, R. Maddalena, T. W. Lane, Low molecular weight volatile organic compounds indicate grazing by the marine rotifer brachionus plicatilis on the microalgae microchloropsis salina. *Metabolites* **10**, 1–20 (2020).
20. E. R. Moore, C. L. Davie-Martin, S. J. Giovannoni, K. H. Halsey, Pelagibacter metabolism of diatom-derived volatile organic compounds imposes an energetic tax on photosynthetic carbon fixation. *Environ. Microbiol.* **22**, 1720–1733 (2020).
21. E. C. Howard, *et al*., Bacterial taxa that limit sulfur flux from the ocean. *Science* **314**, 649–652 (2006).
22. B. R. Miller *et al*., Medusa: A sample preconcentration and GC/MS detector system for in situ measurements of atmospheric trace halocarbons, hydrocarbons, and sulfur compounds. *Anal. Chem.* **80**, 1536–1545 (2008).
23. J. Laskin, A. Laskin, S. A. Nizkorodov, Mass spectrometry analysis in atmospheric chemistry. *Anal. Chem.* **90**, 166–189 (2018).
24. A. G. Harrison, *Chemical Ionization Mass Spectrometry* (Taylor & Francis, ed. 2, 1992).
25. M. J. Kim *et al*., Bacterial-driven production of nitrates in seawater. *Geophys. Res. Lett.* **42**, 1–8 (2015).
26. M. J. Kim *et al*., Air-sea exchange of biogenic volatile organic compounds and the impact on aerosol particle size distributions. *Geophys. Res. Lett.* **44**, 3887–3896 (2017).
27. H. Danner, D. Samudrala, S. M. Cristescu, N. M. Van Dam, Tracing hidden herbivores: Time-resolved non-invasive analysis of belowground volatiles by proton-transfer-reaction mass spectrometry (PTR-MS). *J. Chem. Ecol.* **38**, 785–794 (2012).
28. M. Luchner *et al*., Implementation of proton transfer reaction-mass spectrometry (PTR-MS) for advanced bioprocess monitoring. *Biotechnol. Bioeng.* **109**, 3059–3069 (2012).
29. T. G. Custer, W. P. Wagner, S. Kato, V. M. Bierbaum, R. Fall, Potential of on-line CIMS for bioprocess monitoring. *Biotechnol. Prog.* **19**, 1355–1364 (2003).
30. R. S. Blake, P. S. Monks, A. M. Ellis, Proton-transfer reaction mass spectrometry. *Chem. Rev.* **109**, 861–896 (2009).
31. M. Roveretto *et al*., Real-time detection of gas-phase organohalogens from aqueous photochemistry using orbitrap mass spectrometry. *ACS Earth Space Chem.* **3**, 329–334 (2019).
32. R. Beale, P. S. Liss, J. L. Dixon, P. D. Nightingale, Quantification of oxygenated volatile organic compounds in seawater by membrane inlet-proton transfer reaction/mass spectrometry. *Anal. Chim. Acta* **706**, 128–134 (2011).
33. L. J. Carpenter, S. D. Archer, R. Beale, Ocean-atmosphere trace gas exchange. *Chem. Soc. Rev.* **41**, 6473–6506 (2012).
34. K. H. Halsey *et al*., Biological cycling of volatile organic carbon by phytoplankton and bacterioplankton. *Limnol. Oceanogr.* **62**, 2650–2661 (2017).
35. M. Steiner, T. Hartmann, Über Vorkommen und Verbreitung flüchtiger Amine bei Meeresalgen [in German]. *Planta* **79**, 113–121 (1968).
36. M. C. Facchini *et al*., Important source of marine secondary organic aerosol from biogenic amines. *Environ. Sci. Technol.* **42**, 9116–9121 (2008).
37. D. Pagonis, J. E. Krechmer, J. De Gouw, J. L. Jimenez, P. J. Ziemann, Effects of gas-wall partitioning in Teflon tubing and instrumentation on time-resolved measurements of gasphase organic compounds. *Atmos. Meas. Tech.* **10**, 4687–4696 (2017).
38. X. Liu *et al*., Effects of gas-wall interactions on measurements of semivolatile compounds and small polar molecules. *Atmos. Meas. Tech.* **12**, 3137–3149 (2019).
39. H. Yu, S. H. Lee, Chemical ionisation mass spectrometry for the measurement of atmospheric amines. *Environ. Chem.* **9**, 190–201 (2012).
40. D. Cadena-Herrera *et al*., Validation of three viable-cell counting methods: Manual, semi-automated, and automated. *Biotechnol. Rep. (Amst.)* **7**, 9–16 (2015).
41. M. Bedrossian, C. Barr, C. A. Lindensmith, K. Nealson, J. L. Nadeau, Quantifying microorganisms at low concentrations using digital holographic microscopy (DHM). *J. Vis. Exp.* **2017**, 1–11 (2017).
42. Y. Morono, T. Terada, N. Masui, F. Inagaki, Discriminative detection and enumeration of microbial life in marine subsurface sediments. *ISME J.* **3**, 503–511 (2009).
43. G. Subramanian, S. Shanmugasundaram, Uninduced ammonia release by the nitrogenfixing cyanobacterium Anabaena. *FEMS Microbiol. Lett.* **37**, 151–154 (1986).
44. P. K. Thomas, G. P. Dunn, M. Passero, K. P. Feris, Free ammonia offers algal crop protection from predators in dairy wastewater and ammonium-rich media. *Bioresour. Technol.* **243**, 724–730 (2017).
45. D. M. Metzler, A. Erdem, C. P. Huang, Influence of algae age and population on the response to Tio2 nanoparticles. *Int. J. Environ. Res. Public Health* **15**, 585 (2018).
46. M. M. Allen, Simple conditions for growth of unicellular blue-green algae on plates. *J. Phycol.* **4**, 1–4 (1968).
47. N. G. Schoepp *et al*., System and method for research-scale outdoor production of microalgae and cyanobacteria. *Bioresour. Technol.* **166**, 273–281 (2014).
48. D. Aljawhary, A. K. Y. Lee, J. P. D. Abbatt, High-resolution chemical ionization mass spectrometry (ToF-CIMS): Application to study SOA composition and processing. *Atmos. Meas. Tech.* **6**, 3211–3224 (2013).
49. A. Taton *et al*., Gene transfer in Leptolyngbya sp. strain BL0902, a cyanobacterium suitable for production of biomass and bioproducts. *PLoS One* **7**, e30901 (2012).
50. C. G. Ryan, E. Clayton, W. L. Griffin, S. H. Sie, D. R. Cousens, SNIP, a statistics-sensitive background treatment for the quantitative analysis of PIXE spectra in geoscience applications. *Nucl. Instrum. Methods Phys. Res. B* **34**, 396–402 (1988).
51. P. Wenig, J. Odermatt, OpenChrom: A cross-platform open source software for the mass spectrometric analysis of chromatographic data. *BMC Bioinformatics* **11**, 405 (2010).
52. J. S. Sauer *et al*., Gas composition and fluorescence data for: Continuous Measurements of Volatile Gases as Detection of Algae Crop Health. UC San Diego Library Digital Collections. https://doi.org/10.6075/J0GH9GHW. Deposited 16 September 2021.